Symposium on Applied Aerodynamics and Design of Aerospace Vehicle (SAROD 2011)
November 16-18, 2011, Bangalore, India

ELEVATOR HINGE MOMENT STUDIES OVER GENERIC WINGED BODY CONFIGURATION

M Prasath [*], V R Ganesan[*], A E Sivaramakrishnan[+],
Rajan Kurade[#] and Sambath Rao[#]
Vikram Sarabhai Space Centre, Indian Space Research Organization, Trivandrum, India.

ABSTRACT

Elevator hinge moment measurements have been carried out on a generic wing body configuration through wind tunnel tests. Tests have been carried out at subsonic and transonic Mach numbers in the angles of attack range -4° to 24°. Maximum hinge moment coefficient occurs in the transonic region as expected. Positive deflections of elevator produce higher elevator hinge moment coefficient compared to that of negative deflections. Elevator hinge moment coefficient is linear with elevator deflection up to ±10° and angles of attack up to 10°.

Key Words: Elevator, Hinge moment, Winged-body, Subsonic, Transonic

NOMENCLATURE

α	Angle of attack
HM	Hinge moment
C_{hme}	Elevator hinge moment coefficient
δ	Elevator deflection, deg

1. INTRODUCTION

Wing body configurations use elevator for pitch and roll control. Presently, these control surfaces are operated through actuators. The design of control actuators are very critical, [1] [2] because these actuators must not only withstand the aerodynamic loads but also should accomplish the task of providing the required control throughout the flight envelope.

The prime parameter to be considered in the design of the control actuator is the amount of load acting on the control surface. The aerodynamic force acting on the control surface produces moment about the hinge line and is termed as hinge moment. The hinge moment should be characterized for the range of Mach numbers and control surface deflections through which the vehicle is intended to fly [3]. For the present winged body configuration, the elevators are located at the wing trailing edge and it runs from root to tip. Both starboard and port elevators are used to control the vehicle during its course of flight in pitch and roll.

[*]Scientist/Engineer, Aerodynamics Design Division

[+] Group Head, ACEG/ADTG/AERO

#Scientist, National Aerospace Laboratories, Bangalore

2. TEST DETAILS

Wind tunnel tests have been carried out at subsonic and transonic Mach numbers of 0.3, 0.7, 1.1 and 1.2 at angles of attack (α) ranging from -4° to 24°. The elevator deflections studied are -20°, -10°, 0°, 10° and 20°. The sign convention used for elevator is positive when deflected downward and negative when deflected upward. For the tests, both the elevator are deflected simultaneously either upwards or downwards.

3. TEST FACILITY

Wind tunnel tests are carried out in the 1.2 m Trisonic Wind Tunnel at NAL. This is an intermittent blowdown wind tunnel with a typical run time of about 40 sec. It has a square test section of 1.2 m × 1.2 m. It can be operated from M = 0.30 to 4.0. Transonic Mach numbers are achieved by using a transonic insert, which has perforated walls. The top and bottom walls have 60° inclined holes (12-mm diameter) with an open area ratio 6% and the sidewalls have normal holes (12 mm diameter) with open area ratio 20%. The supersonic Mach numbers are achieved by using a flexible nozzle. The model incidence can be varied from -13° to 27°. The incidence of the model can be varied either in continuous pitch or pitch and pause mode.

4. INSTRUMENTATION

Strain gauges fixed on the hinge line of the elevator are used to measure the hinge moment. Since the strain gauges are mounted directly on the hinge line, the output from the strain gauge is the direct measure of Hinge Moment of the elevator.

Instrumented elevator in which measurements are made is attached to the wing with the help of deflection brackets. Figure 1 and Figure 2 show the CAD model of instrumented elevator. Figure 3 shows that the assembly of the instrumented elevator with the starboard wing. Out of two elevators, only one elevator is instrumented and measurement is made on this instrumented elevator. Torsional stiffeners are provided on either side of elevator to avoid any lateral twist of the elevator during the tests.

The methodology for computing the elevator hinge moment is follows,

- Strain gauges are mounted on the hinge line of the elevator.
- Instrumented elevator is fixed to the wing which acts as a cantilever beam.
- Load experienced by the elevator during the tests is transferred to the hinge line as bending moment which is measured as hinge moment in the model.

5. CALIBRATION

Calibration plays vital role in hinge moment measurements. A general method developed for calibrating strain-gage installations, which permits the measurement of the bending moment and shear forces on the control surfaces are described in Ref [4].

Prior to the tests, instrumented elevator has been calibrated. Known loads are applied at various loading points on the calibration body. The applied hinge moment is obtained by multiplying the load and the distance between the hinge line and loading points. Figure 4 and Figure 5 show the schematic of calibration body with elevator and its sectional view. Top portion of the calibration body have been maintained horizontal before loading. Figure 6 shows the loading points on elevator for calibration. The sensitivity is then obtained by fitting a least square curve in linear sense between the applied hinge moment and the balance output. The mean sensitivity is used to compute the hinge moment data during tests.

6. RESULTS AND DISCUSSIONS

Wind tunnel tests have been carried out at subsonic and transonic Mach numbers to characterize the hinge moment on elevator over generic winged body configuration.

6.1 Elevator Hinge Moment Coefficient at M=0.3

Variations of elevator hinge moment coefficient C_{hme} with α for different elevator deflection at M=0.3 is shown in Figure 7. The wing of the present winged body configuration has reflex aerofoil. A negative normal force is expected at 0° angle of attack. Due to this small amount of negative normal force, a positive elevator hinge moment is experienced at this angle of attack. As the angle of attack increases, the normal force of the elevator increases and hence the hinge moment decreases from positive value to negative value.

Figure 8 gives the variation of Elevator hinge moment coefficient C_{hme} with elevator deflection (δ) at M=0.3 for various angles of attack (α). From the figure it is observed that variation of C_{hme} is linear with Elevator deflection up to ±10˚ and angles of attack up to 10˚ and positive deflections produces higher HM than that of negative deflections. The reason is that the net angle of attack between the free stream and the deflected elevator for positive elevator deflection increases and hence normal force increases resulting increase in hinge moment, whereas for negative deflection, since the net α decreases, normal force decreases resulting decrease in the hinge moment.

6.2 Elevator Hinge Moment Coefficient at M=0.7

Elevator hinge moment coefficients at M=0.7 are shown in Figure 9. The flow features are same as that of M=0.3. The vehicle can be trimmed at α=10˚ for basic configuration and trimable at α=22° for elevon deflected at -10° configuration (i.e. deflected upwards).

6.3 Elevator Hinge Moment Coefficient at M=1.1

Elevator hinge moment coefficients at M=1.1 are shown in Figure 10. For basic configuration, elevator hinge moment coefficient increases up to angle of attack of 22° because of the increase in the normal force coefficient. Beyond that, hinge moment coefficient decreases due to high angle of attack effects. Positive deflection of elevator generates negative hinge moment and vice versa. As the elevator deflection increases, hinge moment also

increases due to increment in the normal force. For positive deflection of elevon, hinge moment coefficient increases as the angles of attack increases. But for negative angles of attack, hinge moment coefficient decreases as the angles of attack increases. This is because of the effect of net angles of attack as discussed earlier.

Figure 11 gives the variation of Elevator hinge moment coefficient with elevator deflection (δ) at M=1.1 for various angles of attack (α). From the figure it is observed that variation of C_{hme} is linear with Elevator deflection up to ±10˚ and angles of attack up to 10˚. It is also observed that the positive deflection of elevator produces higher HM than that of negative deflections.

6.4 Elevator Hinge Moment Coefficient at M=1.2

Figure 12 shows the Elevator hinge moment coefficient at M=1.2 for different angles of attack. The flow features are same as that of M=1.1. Maximum hinge moment coefficient is observed for negative angles of attack for all deflections of elevons. This is because at negative angles of attack, the elevon is in windward region and for positive angles of attack, the elevon is in leeward region.

4. CONCLUSION

Hinge moment tests have been carried out on elevator of a generic winged body configuration in 1.2m Trisonic wind Tunnel, NAL at Mach numbers 0.3, 0.7, 1.1 and 1.2 at α varying between -4° to 24°. Maximum hinge moment coefficient occurs at M=1.1 as expected. Positive deflections of elevator produces higher hinge moment coefficient compared to that of negative deflections. Elevator hinge moment coefficient is linear with elevator deflection up to ±10˚ and angles of attack up to 10˚.

ACKNOWLEDGMENT

The authors acknowledge Head, NTAF, NAL and team for their dedicated model making and wind tunnel tests.

REFERENCES

1. Jerald M J, Ming H T and George P E, “Vertical fin loads and control surface hinge moment measurements on the M2-F2 lifting body during initial subsonic flight tests” NASA TM X 1712.
2. Ming H T and Micheal DeAngelies, “Fin loads and control surface hinge moments measured in full scale wind tunnel tests on the X-24A flight vehicle”, NASA TM X 1922.
3. Hwang W, Chen W, Tasi, P “Measuring Flight Hinge Moment”, AIAA-91-2423.
4. Sknpinski T, Aikcn V . S, Huston T “Calibration of Strain-Gage Installations in Aircraft Structures for the Measurement of Flight Loads”, NACA REP 1178, 1954.

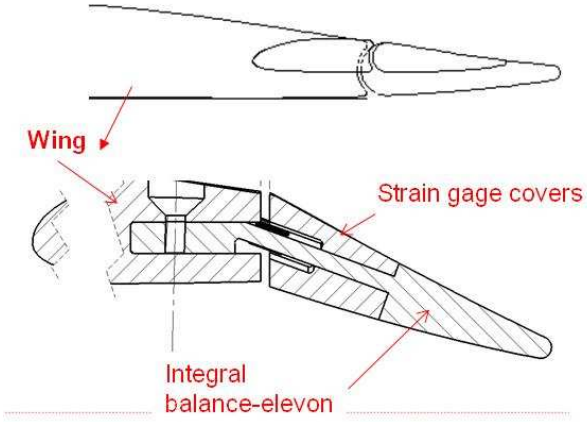

Figure 1. Sectional view of CAD model of instrumented elevator

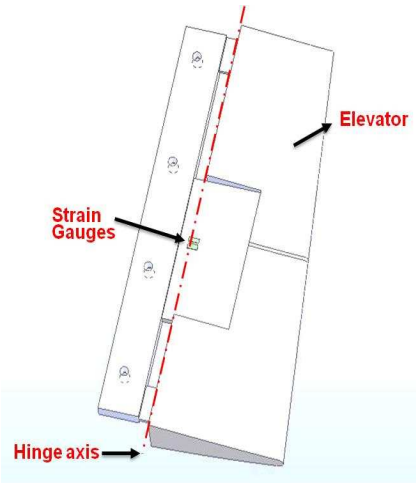

Figure 2. CAD model of instrumented elevator showing hinge axis

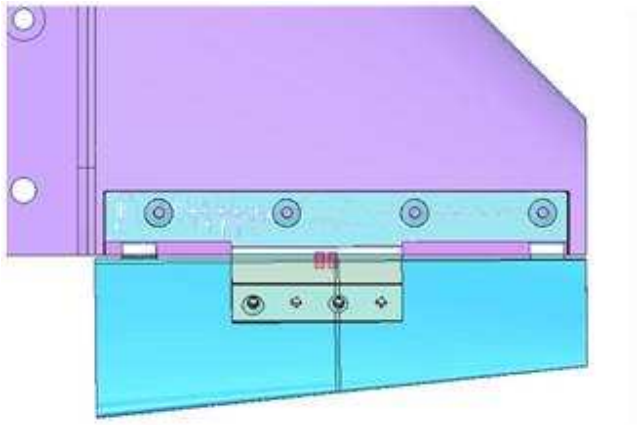

Figure 3. Assembly of elevator with the wing

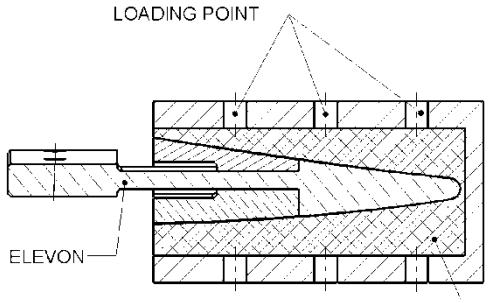

Figure 4. Schematic of Calibration body with elevator(Sectional view)

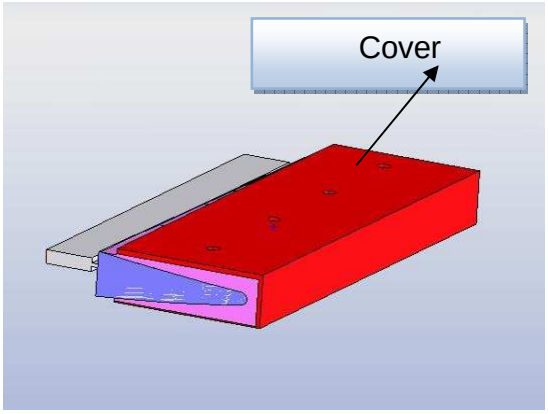

Figure 5. Schematic of Calibration body (3D CAD) with elevator

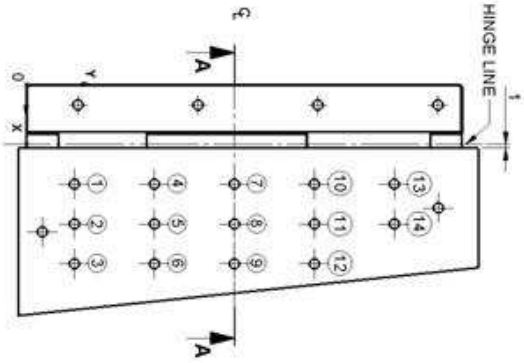

Figure 6. Loading points in Elevator for calibration

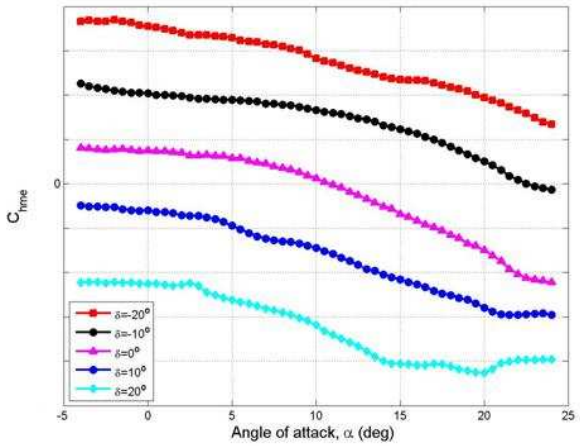

Figure 7. Variation of C_{hme} with α for different elevator deflection (δ) at M=0.3

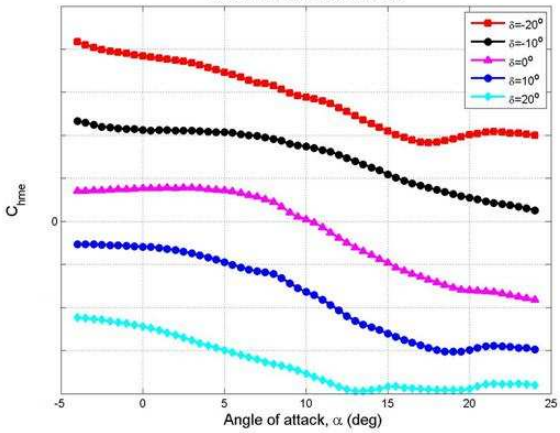

Figure 9. Variation of C_{hme} with α for different elevator deflection at M=0.7

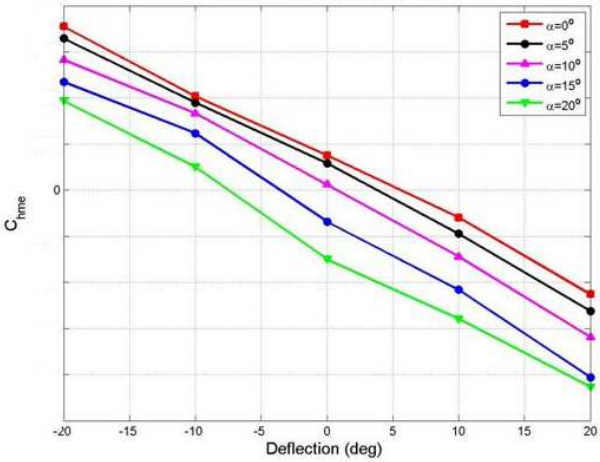

Figure 8. Variation of C_{hme} with δ for different angles of attack (α) at M=0.3

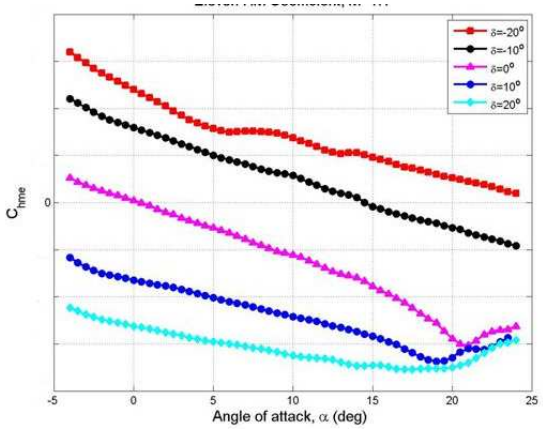

Figure 10. Variation of C_{hme} with α for different elevator deflection at M=1.1

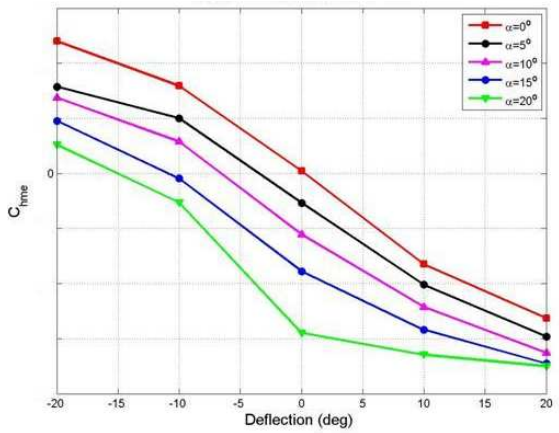

Figure 11. Variation of C_{hme} with δ for different angles of attack (α) at M=1.1

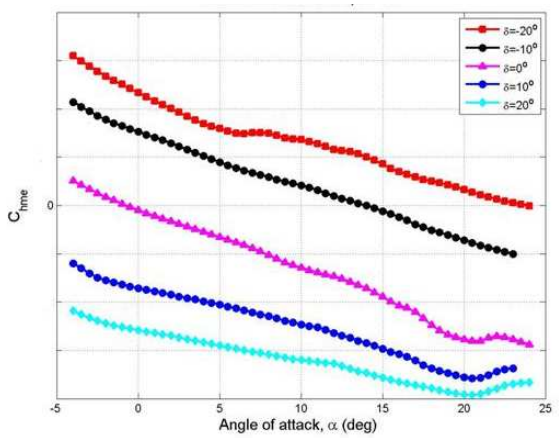

Figure 12. Variation of C_{hme} with α for different elevator deflection at M=1.2